Atmos. Meas. Tech. Discuss., 8, 7057–7091, 2015
www.atmos-meas-tech-discuss.net/8/7057/2015/
doi:10.5194/amtd-8-7057-2015

Atmospheric Measurement Techniques
Discussions
Open Access

# Study of the regional $CO_2$ mole fractions filtering approach at a WMO/GAW regional station in China

**S. X. Fang[1], P. P. Tans[2], M. Steinbacher[3], L. X. Zhou[1], and T. Luan[1]**

[1]Chinese Academy of Meteorological Sciences (CAMS), China Meteorological Administration (CMA), Beijing, China
[2]Earth System Research Laboratory (ESRL), National Oceanic and Atmospheric Administration (NOAA), Boulder, CO, USA
[3]Empa, Swiss Federal Laboratories for Materials Science and Technology, Laboratory for Air Pollution/Environmental Technology, Duebendorf, Switzerland

Received: 28 May 2015 – Accepted: 18 June 2015 – Published: 10 July 2015

Correspondence to: S. X. Fang (fangsx@cams.cma.gov.cn)

Published by Copernicus Publications on behalf of the European Geosciences Union.

## Abstract

The identification of atmospheric $CO_2$ observation data which is minimally influenced by very local emissions/removals is essential for the estimation of trend analysis, regional sources and sinks, and for modeling of long-range transport of $CO_2$. In this study, four approaches are used to filter the atmospheric $CO_2$ observation records from 2009 to 2011 at one World Meteorological Organization/Global Atmosphere Watch (WMO/GAW) regional station (Lin'an, LAN) in China. The methods are based on the atmospheric black carbon concentration (BC), on a statistical approach (REBS), on $CH_4$ as auxiliary tracer (AUX) and on meteorological parameters (MET). All approaches do suitably well to capture the seasonal $CO_2$ cycle at LAN. Differences are observed in the average regional mole fractions with annual values in the REBS method at least $1.7 \pm 0.2$ ppm higher than the other methods. The BC method may underestimate the regional $CO_2$ mole fractions during winter-spring period and should be treated with caution. The REBS method is a purely statistical method and it may also introduce errors on the regional $CO_2$ mole fractions evaluations, as the filtered trend may be deviated by the "noisy" raw data series. Although there are correlations between $CH_4$ and $CO_2$ mole fractions at LAN, the different source/sink regimes may introduce bias on the regional $CO_2$ estimation in the AUX method, typically in summer. Overall, the MET method seems to be the most favorable because it mainly focuses on the influence of potential local sources and sinks and considers diurnal variations, local topography, and meteorological conditions. Using the MET method, the annual growth rate of regional $CO_2$ at LAN is determined to be $3.1 \pm 0.01$ ppm $yr^{-1}$ (standard error) from 2009 to 2013.

## 1 Introduction

Carbon dioxide ($CO_2$) is the most important greenhouse gas in the atmosphere. It contributes more than 60 % of total Radiative Forcing (RF) of the long-lived greenhouse gases (AGGI, 2014). The large increase of atmospheric $CO_2$ of nearly 120 ppm above preindustrial levels has been unequivocally attributed to human emissions (Keeling, 1993; WMO, 2014). Using atmospheric $CO_2$ observations, the source/sink estimations can be constrained through inverse models, which is an important way to understand the carbon cycle in the land biosphere (Chevallier et al., 2011; Thompson et al., 2009). For this purpose, lots of ground-based stations have been set up to monitor the $CO_2$ mole fractions around the world. So far, there are more than 150 sites worldwide where greenhouse gas mole fractions are measured (Artuso et al., 2009; Dlugokencky et al., 1995; Necki et al., 2003; Sirignano et al., 2010; Tans et al., 1990; WMO, 2014). Due to technical constraints like access to the measurement site, power supply or internet connection, very few monitoring stations are always exposed to pristine air masses while many GAW stations are occasionally to frequently affected by local sources or sinks (Tsutsumi et al., 2006; Riley et al., 2005). The measurements at the majority of sites cannot fully represent the well-mixed $CO_2$ conditions in the regions. Hence data filtering is an essential part for the analysis of data from those sites when trying to retrieve representative trends, for sources and sinks estimations or for modeling of long-range transport of trace gases (Greally et al., 2007; Novelli et al., 2003; Prinn et al., 2001; Ryall et al., 1998).

Several methods have been applied in the past for the extraction of background (or regionally representative) ground based measurements. (1) Filters based on specific trace gases or ratios of trace gas - trace gas. For example, Tsutsumi et al. (2006) used carbon monoxide (CO) as an indicator to filter the observed $CO_2$ mole fractions at Yonagunijima station located in East Asia. Zanis et al. (2007) used the total reactive nitrogen ($NO_y$) to CO ratio to distinguish different regimes at the high-altitude station Jungfraujoch in Central Europe. Brunke et al. (2004) used Radon and CO to classify their observations at Cape Point, South Africa. (2) Meteorological filters, which are the most commonly used. This method can e.g. consider various factors such as the local wind speed, wind direction, boundary layer heights, information on the atmospheric stability, solar input, or weather statistics and others but also the diurnal $CO_2$ variation as it can be closely linked to the above parameters (Artuso et al., 2009; Chmura et al., 2008; Collaud Coen et al., 2011; Zellweger et al., 2003; Zhou et al., 2005). Frequently this method integrates two or more of the above factors to extract the regionally representative conditions. (3) Statistical methods. This approach generally uses the variations (e.g. a low standard deviation) of observed data in certain time windows as a threshold to select the regional values (Cunnold et al., 2002; Morimoto et al., 2003; Zhang et al., 2007). (4) Numerical transport methods, which use atmospheric dispersion modeling (e.g. air mass back trajectories) to study the advection regimes with subsequent distinction in periods with potential influence of local or regional source/sink and uninfluenced conditions (Cape et al., 2000; Manning et al., 2011; Ryall et al., 2001). Some of the studies combined two or more methods above to select the best well-mixed $CO_2$ mole fractions (e.g. Thoning et al., 1989). However, due to the different characteristics of each station such as location (e.g. continental sites, coastal sites), topography, proximity to biosphere and diffuse or point sources etc., the best data filtering approach has to be carefully selected for each station (Ruckstuhl et al., 2012). One method can be also more useful than another at the same station depending on the time series parameter of interest. In brief, there is not a standard method for selecting the background mole fractions from a continuous data series.

With the rapid development of its economy, China has become the largest fossil fuel $CO_2$ emitter in 2006 and emitted 1.8 Pg C in 2011 (LeQuéré et al., 2013; Marland, 2012). The Yangtze Delta area is one of the most developed regions in China and is one of the largest global $CO_2$ emission regions (Gregg et al., 2008). The total population in this area was ~ 159 million in 2010 (National Bureau of Statistics, 2011). Moreover, this area is a highly productive region for paddy rice and winter-wheat in China, which strongly influence the atmospheric $CO_2$ and the variations. For example, winter wheat and rice production in this region represent 20 % of the total Chinese wheat harvest and 5 % of the entire Chinese grain production (Colby et al., 1992; Yan et al., 2003). To understand the character and the abundance of greenhouse gases in this region, the Chinese Meteorological Administration (CMA) has developed the Lin'an (LAN) station in center of the Yangtze Delta area since 1983. The station has been included in the World Meteorological Organization/Global Atmosphere Watch (WMO/GAW) as a regional station and is named after the small town of Lin'an, which is approximately 6 km southwest. There was no in-situ $CO_2$ measuring system until in January 2009, when a Cavity Ring Down Spectrometer (G1301, Picarro Inc.) was installed to continuously monitor atmospheric $CO_2$ and $CH_4$ mole fractions. It was since then we have been acquiring the first-hand greenhouse data at this station (Fang et al., 2013; Pu et al., 2014).

We have found that the $CO_2$ mole fractions at LAN were the highest out of the four WMO/GAW stations in China (Liu et al., 2009; Fang et al., 2011). Based on the meteorological methods, we filtered the $CO_2$ records from 2009 to 2011 and estimated that 16.6 % of the data is likely to be regionally representative (Fang et al., 2014). However, Pu et al. (2014) used black carbon as a chemical tracer to identify the influence of anthropogenic emissions and found that 27.3 % of the data were regionally representative. In a previous study (Fang et al., 2011), we also applied a purely statistical method to filter the data and resulted in regionally representative conditions during 63.5 % of the time in 2009. The different data filtering approaches have induced different results on the regional $CO_2$ mole fractions. Our previous study (Fang et al., 2014) got an average regional $CO_2$ mole fraction of 404.2±3.9 ppm in 2011 at LAN, while Pu et al. (2014) estimated the corresponding average value of 407 ± 5.3 ppm during the same period. The large difference (∼ 3 ppm) between these two methods will definitely induce large bias on the estimation of $CO_2$ abundances in the regional scale as well as on the calculation of source/sink by inverse models. In this paper, we applied four approaches to filter the observed data from 2009 to 2011 at LAN station, and studied the applicability of them. The four methods are black carbon as tracer, a statistical method, methane ($CH_4$) as tracer, and the use of meteorological parameters.

## 2 Experiment

### 2.1 Measurement system

The LAN station (119°44′ E, 30°18′ N, 138.6 m a.s.l.) is about 50 km from Hangzhou (Capital of Zhejiang Province) and 150 km from Shanghai (the largest economic center and the second largest population city in China) (Fig. 1). North of the station (1.4 km away) is a small factory where charcoal is manufactured from bamboo wood. The Lin'an town (with a population of ∼ 100 000) is approximately 6 km southwest to the station. The observatory is built on the top of a small hill and is surrounded with hilly lands and farming areas, with heavy vegetation coverage. The site is located in a humid subtropical monsoon climate zone with mean annual precipitation of 1480 mm and a mean temperature of 15.3 °C.

A Cavity Ring Down Spectrometer (CRDS; Picarro Inc., model G1301) is used for continuous measurements of atmospheric $CO_2$ and $CH_4$. This type of instrument has been proven suitable for making precise measurement of $CO_2$ and $CH_4$ mole fractions since its response is both highly linear and very stable (Chen et al., 2010; Crosson, 2008). The factory reported precision of the instrument is 50 ppb for $CO_2$ and 0.7 ppb for $CH_4$ ($1\sigma$) in 5 min. Sample air is drawn from about 10 m above the ground (agl) regularly. At the end of 2010, a new sampling tower (50 m a.g.l.) was built. At that time, another sampling port was installed at the 50 m. The Picarro system then switched the air sample stream between the 10 m and the 50 m intake every 5 min. The sample air is conditioned and dried to meet the high quality target of the WMO/GAW network. Details of the system are described in Fang et al. (2013). Two standard gases are used to correct the measurements and a target gas is used to check the precision of the system routinely. All of the standards are linked to the WMO X2007 scale (Zhao and Tans, 2006). The CRDS system responds quickly to the sample and reports data with a frequency of 0.3 Hz. For the long-term time series ambient air data is recorded as 5 min averages. Excluding the periods of system maintenance and calibration, more than 97 % of the total 5 min average data points were retained. After computing the

Title Page
Abstract Introduction
Conclusions References
Tables Figures
◀| |▶
◀ ▶
Back Close
Full Screen / Esc
Printer-friendly Version
Interactive Discussion

$CO_2$ mole fractions, the data were manually inspected to flag the analytical or sampling problems. More than 97 % of the 5 min data remained after this filtering step. Then the data were aggregated to hourly averages for further study. Except when noted differently, the averaged values in this study are reported with 95 % confidence intervals (CI). The $CO_2$ concentrations are atmospheric $CO_2$ dry air mole fractions.

## 2.2 Data filtering approach

There are significant $CO_2$ diurnal variations at LAN in all seasons, indicating the strong influence of biological activities near the site including the absorptions by photosynthesis and emissions by plant and soil, and the variation of boundary layer height. The $CO_2$ differences between the parallel measurements (10 and 50 m a.g.l.) at LAN also showed distinct diurnal variations with the stable and minimum values (less than 0.2 ± 0.2 ppm) occurring from 10 to 16 (Local time, LT). At remote sites where the local sources and sinks are sparse, the $CO_2$ diurnal variations are generally weak (e. g. Keeling et al., 1976; Zhou et al., 2005). Thus, in this study, the $CO_2$ data from 10:00 to 16:00 LT were first selected to represent better mixed conditions. Then the selected data were used for the filtering approaches study. We adopted four data selection methods to filter the selected $CO_2$ mole fractions. They are described as follows:

Black carbon tracer (abbreviation: BC). We adopt the similar routine used by Pu et al. (2014). The observed $CO_2$ was filtered based on the observation of both black carbon concentration and meteorological parameters. Pu et al. (2014) found a correlation coefficient of 0.53 ($R$) between black carbon concentrations and $CO_2$ mole fractions and concluded that both $CO_2$ and black carbon have some common sources such as fossil fuel combustion and biomass burning within this area. Thus, first we excluded the episodes when the black carbon concentration was exceeding 5000 ng $m^{-3}$. During the wet season precipitations when the black carbon concentration was very low, we used air mass back trajectory analysis to further flag the data which were likely influenced by anthropogenic emissions from cities nearby. Finally, we studied the average standard deviations ($\sigma$) of hourly $CO_2$ mole fractions as a function of wind speed using all data from 10:00 to 16:00 LT from 2009 to 2011. As shown in Fig. 2, the average $\sigma$ decreased sharply when local surface wind speed was faster than 1.5 $\mathrm{m\,s^{-1}}$. Clearly, higher local surface wind caused better mixed conditions and consequently more stable $CO_2$ mole fractions. Thus the remaining data were further flagged when surface wind speed was below 1.5 $\mathrm{m\,s^{-1}}$ to minimize the influence of very local sources and sinks.

Statistical method (abbreviation: REBS). Here we applied the Robust Extraction of Baseline Signal (REBS) to extract the regional $CO_2$ mole fractions, which was similar to those used in the Global Atmospherics Gases Experiment/Advanced Global Atmospherics Gases Experiment (GAGE/AGAGE) network (Ruckstuhl et al., 2001) to filter halocarbons and other non-$CO_2$ gases. Ruckstuhl et al. (2012) suggested a meteorological filtering of the data should be applied prior to the application of the REBS method, as the polluted conditions might induce a bias on the background classification. In this study, this was taken into consideration by using data from 10:00 to 16:00 LT. The REBS method is a purely nonparametric technique and assumes that the background signal varies very slowly relative to contributions of the regional signal. The observed concentrations $Y(t_i)$ are defined by regional concentration $g(t_i)$ plus polluted concentration $m(t_i)$ plus the measurement errors $E_i$. The measurement errors $E_i$ are assumed to be independent and Gaussian-distributed with mean 0 and variance $\sigma^2$. If the regional signal $m(t_i)$ is zero in a time period around to $t_0$, the baseline signal $g(t_0)$ can be estimated even when the form of the curve $g$ is unknown. The curve $g(t_i)$ is approximated as linear in a sufficiently small neighborhood around any given time point $t_0$. Details of the method are described by Ruckstuhl et al. (2012). A bandwidth of 60 days was used in this study while other bandwidths 90, 120, and 180 days were also tested. The bandwidth choice did not considerably influence the retrieved averages and trends of the regionally representative $CO_2$ mole fractions were similar. In comparison with other methods, this approach did not have to be considerably adapted to the conditions at individual measurement site.

Auxiliary tracer (abbreviation: AUX), which uses $CH_4$ as an auxiliary indicator to filter the $CO_2$ time series. Many previous studies found positive correlations (mostly in winter) between the atmospheric $CH_4$ and $CO_2$ mole fractions (Conway et al., 1989; Tohjima et al., 2014; Wong et al., 2014; Worthy et al., 2009) as well as the respective fluxes from ecosystems (Jamali et al., 2013; Repo et al., 2007). For the data series of $CO_2$ and $CH_4$ at LAN, we also observed an apparent correlation between them during the observing period (Fig. 3). The correlation coefficient ($R$) is higher than 0.5 for all seasons, which indicates that there are similar patterns of $CO_2$ and $CH_4$ sources. This phenomenon is more distinct in spring ($R = 0.7$) and winter ($R = 0.8$) when the photosynthetic activity of the vegetation, i.e. the $CO_2$ uptake is weak. In summer and autumn, the active absorption of $CO_2$ by the terrestrial ecosystem may partly alter the $CO_2$–$CH_4$ correlation. Indeed, the positive coefficients still suggest that the anthropogenic emissions are dominating the carbon cycle at LAN station. In remote areas, an uncorrelated or negatively correlated relationship is generally observed (e. g. Necki et al., 2003). As described above, we also used the Robust Extraction of Baseline Signal (REBS) method to filter the $CH_4$ data because it has proved to be suitable for extracting the background mole fractions of $CH_4$ at remote sites (Cunnold et al., 2002). By doing so, we flagged the hourly $CO_2$ records corresponding to the periods of locally influenced or regionally representative events of $CH_4$ filtered in the REBS method. Moreover, although there were correlations between the atmospheric $CH_4$ and $CO_2$ in all seasons at LAN, they were not perfectly correlated, meaning that some $CO_2$ events could not be determined by $CH_4$ mole fractions. To reduce this influence, we further flagged the $CO_2$ data which deviated from the linear fits by more than $1\sigma$ in the respective season into local events. This additional filter excludes most events with poor $CH_4$–$CO_2$ correlation (Fig. 3).

Meteorological method (abbreviation: MET). As used in previous studies, the diurnal variation of $CO_2$ mole fractions, local surface wind direction, local surface wind speed and the nearby terrain were all considered for the $CO_2$ data filtering (Fang et al., 2014; Zhou et al., 2004, 2005). According to the nearby potential contamination sources (nearby villages, industry etc.), the data when local surface winds were from SSW-SW and N sectors were excluded. Then the data were further flagged by discarding the events when the local surface wind speed was lower than 1.5 m s$^{-1}$ to minimize the influence of very local sources or sinks as discussed above.

After the multiple steps filter, there were still very few discrete data points remaining with high/low $CO_2$ mole fractions in the BC, AUX, and MET method. These odd outliers unlikely represented regional $CO_2$ conditions as they should not spike within few hours. Thus we used a mathematical method to further flag the remainders of data in the BC, AUX, and MET method. The $\sigma$ of hourly $CO_2$ data in a 60-days bandwidth (similar to the REBS method) was calculated. The differences between every data point and the 60 day average were calculated. Data were flagged and excluded if the difference exceeded $3\sigma$. We used the method of Thoning et al. (1989) to extract the $CO_2$ seasonal cycles in the four methods. However, it was recently reported that this method was very sensitive to the outliers in the data series (Pickers et al., 2015). Thus this step also helped to reduce the bias on the seasonal cycle estimation. After that, the remaining data in the BC, AUX, and MET were considered as the least influenced by local sources or sinks.

## 3 Results

### 3.1 Filtered $CO_2$ events

Figure 4 illustrates the filtered $CO_2$ results in the four approaches. From the top to bottom are the results of the BC, REBS, AUX and MET method, respectively. The filtered regional mole fractions account for ~ 12.2 % in BC, 15 % in REBS, 12.8 % in AUX and 16.5 % in MET of the total valid hourly data. The low proportions of regional $CO_2$ in the four methods reflect the strong influences of local sources and sinks. The overall seasonal patterns of regional $CO_2$ retrieved in the four approaches are similar with peaks in winter and troughs in summer, which are consistent with other observations in the Northern Hemisphere (Nevison et al., 2008).

Table 1 illustrates the annual regional $CO_2$ mole fractions in the four methods. The annual mole fractions in the REBS method are apparently higher than the others with the smallest discrepancy at 1.7 ± 0.2 ppm in 2010. As the REBS method uses a purely mathematical method, the high $CO_2$ mole fractions induced by local sources may enhance the $\sigma$ values and enlarge the "regional" $CO_2$ band, and subsequently introduce higher regional $CO_2$ values. The annual $CO_2$ all display increasing trends. Although the annual $CO_2$ determined by the BC method increases from 402.0 ± 0.1 in 2010 to 402.7 ± 0.2 ppm in 2011, the amplitude of increase is so small compared to other years and methods. In fact, the long-term trend in the BC method (polynomial part of the curve fitting function) decreases from February in 2011 (data not shown). Considering the annual growth rate of $CO_2$ with value of ~ 2 ppm from 2010 to 2012 on the global scale (WMO, 2013), and the increasing emissions of $CO_2$ from fossil-fuel combustion in China (CDIAC, 2015), it is unlikely that the regional $CO_2$ mole fractions at LAN almost remained constant from 2010 to 2011.

## 3.2 Comparison of regional $CO_2$ events

We used the curve fitting method described by Thoning et al. (1989) to get the seasonal $CO_2$ trends based on the regional $CO_2$ events from 2009 to 2011 (Figs. 4 and 5). The data were fitted into a function with 3 polynomial terms for the long term trend and 4 annual harmonic terms. To minimize the influences of inconsistent records in the four methods, the data were fitted and interpolated with the same time interval (2 h). For comparison, calculated surface $CO_2$ mole fractions at similar latitude from the Marine Boundary Layer (MBL) reference computed by NOAA/GMD (sine of 0.5, i.e. 30° N) are also presented (MBL, 2015). The monthly $CO_2$ mole fractions in the four methods are apparently higher than the MBL values during the whole year, with an average difference of 10.9 ± 0.1 for BC, 13.9 ± 0.2 for REBS, 11.2 ± 0.2 for AUX and 11.5 ± 0.2 ppm for MET. The large difference indicates that the Greater Yangtze Delta area is an important source of atmospheric $CO_2$. The monthly $CO_2$ variations in the four approaches show similar patterns with minimum values in August and maximum values in December. The appearance of the lowest values matches with the minimum of the MBL reference. As reported in a previous study (Fang et al., 2014), the highest $CO_2$ difference with the Northern Hemisphere at LAN was in December, and was due to the lower boundary layer in winter, as well as the increase of fossil fuel consumption (partly for domestic heating) and cement burning, as well as plant respiration. In general, these four approaches are doing well to capture the seasonal $CO_2$ cycles at LAN station.

However, there are also differences between the monthly $CO_2$ mole fractions. The monthly $CO_2$ values in the REBS method are always higher than the other methods (Fig. 5a). This is because the REBS method uses variations of the raw data (standard deviation) as a threshold to flag the locally influenced $CO_2$ mole fractions. The "noisy" $CO_2$ mole fractions (mostly high outliers) may draw the trend of regional events upward and subsequently induce higher regional values. This result also indicates that the REBS method may be less suitable for the $CO_2$ data filtering at LAN. In fact, this method is mostly used at remote sites with few local sources and sinks (e.g. Zhang et al., 2013).

During the winter-spring period, the regional $CO_2$ mole fractions retrieved with the BC method are apparently lower than the other methods. It is because the BC method mainly refers to the measured black carbon concentrations. Emissions of black carbon and $CO_2$ from fossil fuel and biomass burning occur at both the local and regional scale (Baumgardner et al., 2002), and the BC method robustly flags the $CO_2$ mole fractions when black carbon concentrations exceed the threshold value ($5000\,\mathrm{ng\,m^{-3}}$). However, it is difficult to distinguish the local emissions of black carbon from the regional contents. Especially during the winter-spring seasons, the regional black carbon and $CO_2$ concentrations are both high due to the increase of fossil fuel consumption and cement burning (Feng et al., 2014). These high concentrations should still represent the volumes at regional scale and should not be flagged. Thus in the BC method, the flagging of higher $CO_2$ mole fractions into local representatives is probably the reason for the lower regional $CO_2$ values during the winter-spring period. Secondly, the BC method mainly geared to the polluted air masses altered by anthropogenic sources, and the influence of land biosphere in the daytime remains unconsidered. Moreover, the large difference of the lifetime, which is 4–12 days for black carbon (Cape et al., 2012) and more than decades for $CO_2$ (Moore and Braswell, 1994), may also contribute to the bias of this method.

The monthly $CO_2$ mole fractions in the AUX method are lower than in the other methods in summer. During this time of the year, a large amount of $CH_4$ is emitted from wetlands (e.g. rice paddy fields) on the eastern China plain (Lu et al., 2000; Zhang et al., 2010). Thus, these high values should represent regional conditions rather than local events (Fang et al., 2013). On the contrary, the active processes of photosynthesis by local and regional vegetation in summer reduce the observed $CO_2$ mole fractions, especially by local vegetation, which has a strong negative influence on the $CO_2$ mole fractions during afternoon. This influence can also be seen from the frequently lower $CO_2$ mole fractions at 10 m a.g.l. than at 50 m a.g.l. in the daytime. These different source/sink regimes may cause some flagged “regional” $CO_2$ mole fractions which are actually influenced by the absorption of local vegetation, subsequently leading to lower regional values in summer.

Compared with the BC, REBS, and AUX method, there is no apparent disadvantage for the MET method, as it mainly concerns on the possible influence of local sources and sinks combined with the meteorological conditions. Figure 5b illustrates the detrended seasonal cycles of $CO_2$ in the four approaches. The peak to trough amplitudes of regional $CO_2$ are $14.4 \pm 0.1$, $18.6 \pm 0.1$, $22.7 \pm 0.1$ and $20.4 \pm 0.1$ ppm for the BC, REBS, AUX and MET method, respectively. The amplitude for the BC method is the lowest, which is ascribed to the lower $CO_2$ mole fractions during the winter-spring period, and the higher values than AUX and MET method in summer. The higher $CO_2$ mole fractions in the BC method in summer may be due to the lower black carbon concentrations (Feng et al., 2014). The highest $CO_2$ amplitude is observed in the AUX method, which is ascribed to the lowest $CO_2$ mole fractions in summer.

The regional $CO_2$ mole fractions all show positive trends with annual growth rates of 1.8 ± 0.01 for BC, 2.8 ± 0.01 for REBS, 3.2 ± 0.01 for AUX and 3.1 ± 0.01 ppm $yr^{-1}$ (standard error) for MET. According to the statistics results from the WMO greenhouse Gas Bulletins (2012, 2013; 2014), the global $CO_2$ increasing rate exceeded 2 ppm from 2009 to 2012. The growth rate for the BC method is lower than the global average, which may partly be caused by the different $CO_2$ to black carbon patterns over the considered years. As the regional $CO_2$ value in the BC method is based upon the black carbon concentrations, the increasing fossil fuel standards (upgraded from Chinese national stage 3 to 4 since 2010) and exhaust efficiency may induce different patterns between $CO_2$ and black carbon concentrations and hence extract a smaller $CO_2$ growth rate. Similar to the annual $CO_2$ mole fractions (Table 1), the annual growth rates of the AUX and MET method are close. It should be mentioned that only three years are used to evaluate the annual $CO_2$ growth rate. The relative short time series here may inevitably induce bias on the growth rate estimation, which need to be treated with caution.

### 3.3 Comparison of local $CO_2$ events

The benefit of a successful extraction of regional values is two-fold. The identified regional values can be used e.g. for the determination of regionally representative trends. On the other hand, the data considered to be locally influenced can be used to learn more about the sources and sinks in the vicinity of the station. Figure 6a displays the seasonal variations of local $CO_2$ mole fractions in the four approaches. The data were also fitted and smoothed by the method of Thoning et al. (1989). The local $CO_2$ events all reveal a broad spring maximum peaking in May and a distinct winter maximum with highest value in December. Minimum values are all observed in August. The peak in December and valley in August agrees with the seasonal pattern of the regional data. However, there is another distinct peak in May in all the approaches. Feng et al. (2014) observed the black carbon in Shanghai, China (150 km to LAN) and found three peaks of January–February, April–June, and November–December from 2010 to 2011. As the anthropogenic emissions of black carbon and $CO_2$ in the Yangtze area have a similar spatial distribution (Qin et al., 2012), the peaks in May and December are probably due to the anthropogenic emissions. On the other hand, the peak in May is blurred due to the dampening effect caused by the $CO_2$ uptake with the onset of the growing season.

Except from December to January, the local $CO_2$ mole fractions in the BC method are always higher than the other methods. As discussed above, the tendency of flagging higher $CO_2$ mole fractions into local representatives is probably the main reason for the higher $CO_2$ values. This result also indicates that the BC method induces bias on the local $CO_2$ estimations. However, it should be mentioned that there is not a negative correlation between the regional and local $CO_2$ mole fractions in these methods. For example, the regional $CO_2$ in the REBS method are generally higher than the other methods, but the local $CO_2$ are not apparently lower than the AUX and MET method (Fig. 6a). Although the regional $CO_2$ "band" in the REBS method (blue dots in Fig. 3) is higher than the other methods, and the average local $CO_2$ mole fraction above this band is larger, a considerable proportion of local $CO_2$ mole fractions (below the regional band in Fig. 3) flagged as absorption by local sinks (e.g by photosynthesis of local vegetation) pulls the fitted curved down and consequently induces similar seasonal local $CO_2$ patterns with the AUX and MET method.

Meteorological data (such as surface wind direction and speed) could help to understand the greenhouse gases emission and transport (Dlugokencky et al., 1995; Massen and Beck, 2011). Figure 6b shows the wind-rose distribution patterns of local $CO_2$ mole fractions in the four methods. The distributions are similar with higher $CO_2$ values on SW-SSW sectors. This is due to the anthropogenic emissions from the Lin'an town located at approximately 6 km southeast of LAN (Fig. 1). The local $CO_2$ mole fractions on the WSW to SSW sectors in the BC method are apparently higher than in the other methods. It is also probably due to the tendency of flagging higher $CO_2$ mole fractions emitted from the town. The local $CO_2$ mole fractions on these sectors in the MET method are also higher than those of the REBS and AUX method. Actually, we studied the wind-rose $CO_2$ distributions in different seasons and found most of the discrepancies occurred in summer. This phenomenon can also be seen from Fig. 6a with higher values in the MET method than AUX and REBS method in August. As discussed above, the lower local $CO_2$ mole fractions in the AUX and REBS method in summer are probably due to the local $CO_2$ mole fractions (below the regional band in Fig. 3) flagged as absorption by local sinks (e.g. by photosynthesis of local vegetation).

### 3.4 Case analysis

To further investigate the difference of the four data filtering approaches, we used a period in winter as a case study. As in winter, $CO_2$ mole fractions at LAN are pretty high due to the strong emissions and weak absorption by the regional terrestrial ecosystems. Here we selected two time phases which were from 06:00 to 16:00 LT on 29 December 2010 (phase 1) and 30 December 2010 (phase 2), respectively (see Fig. 7). Phase 1 features elevated $CO_2$ mole fractions while phase 2 reveals "normal" $CO_2$ values. We compute the 3 day back trajectories with 500 m a.g.l. for the period with elevated $CO_2$ (28 December 2010 19:00 LT to 29 December 2010 06:00 LT) using the Hybrid Single – Particle Lagrangian Integrated Trajectory (HYSPLIT) dispersion model (Draxler and Rolph, 2003). The model is based on NCEP/NCAR reanalysis data and the trajectories were calculated for every hour (01:00, 02:00, 03:00 LT,...). Figure 8 shows all calculated trajectories in phase 1. It can be seen that almost all of the air mass reaching LAN were transported over Hangzhou city (Province of Zhejiang province, ~ 50 km east to the station) and Nanjing city (province of Jiangsu province, ~ 230 km north to the station). The black carbon during this period also displays an increased concentration. Since black carbon is mainly emitted by fossil fuel combustion and biomass burning (Penner et al., 1993; Cooke and Wilson, 1996), the enhanced $CO_2$ mole fractions should be mainly caused by the transport of emissions from these cities. Both the BC and AUX method flag all data in phase 1 as locally influenced (Fig. 7). In the BC method, due to the increased black carbon concentration, all the $CO_2$ data are flagged because the black carbon concentrations are apparently higher than the yearly average. The meteorological conditions from 10:00 to 16:00 LT in phase

1 favor dilutions, i.e., average surface wind speed is 2.6 m s$^{-1}$; the $\sigma$ of the hourly mole fractions is less than 1.3 ppm. Although the $CO_2$ mole fractions increased in this phase, it was more likely influenced by regional sources (e.g. from Hangzhou and Nanjing) rather than local sources. Thus, the BC and AUX method may erroneously assign local conditions. In phase 2, some data points from 10:00 to 16:00 LT are flagged as regional except in the REBS method. As discussed above, this method is a purely statistical method. The existence of frequently high mole fractions in winter may enlarge the $\sigma$ and may consequently deviate the regional events from the real trend. As a result, some low "regional" $CO_2$ mole fractions as in phase 2 may not be identified.

## 4 Discussions and conclusions

The main purpose of data filtering at a regional station is to identify the data which are least influenced by local sources and sinks (Tsutsumi et al., 2006). However, due to the unique conditions for each station (i.e., topography, air mass transport, economic development level, etc.) and the complex influences of local sources and sinks, there is no ultimate way to absolutely distinguish the locally influenced $CO_2$ from the original data series. Thus data filtering at this type of regional station is a relatively "arbitrary" work. In this study, four data filtering approaches are used to flag the observed data from 2009 to 2011 at Lin'an (LAN) station in the Yangtze Delta area, China. Each of the methods applies multiple steps to flag the observed $CO_2$ mole fractions. The strong diurnal variations of observed $CO_2$ mole fractions and the discrepancy between the parallel measurements (10 and 50 m a.g.l.) indicates that selecting daytime data only is the first and critical step to study $CO_2$ mole fractions at this kind of station. The four methods in this study are suitable to capture the seasonal cycles of regional $CO_2$ at LAN, however, the different regimes in these methods also induce bias on the regional or local mole fractions evaluations.

The BC method may be treated with caution, as it is difficult to distinguish the local emissions of black carbon with the regional contents. Especially during the winter-spring seasons, this method may underestimate the regional $CO_2$ mole fractions at LAN. Moreover, it mainly gears to the polluted air masses altered by anthropogenic sources, and does not consider the influence of the land biosphere. Additionally, the different lifetime between atmospheric $CO_2$ and black carbon may also introduce errors on the estimation. In this study, the annual mole fractions, the annual growth rate, and the local $CO_2$ values in the BC method are different with the other three methods.

The REBS method is based on a purely statistical method. This method is appealing as it requires no additional information (site specific criteria, additional observations). However, it may also induce errors when evaluating the regional $CO_2$ mole fractions, e.g. overestimating the regional values. Due to the "noisy" $CO_2$ mole fractions at the regional sites like LAN, the filtered regional trend may be drawn upward or pulled down from the real variation.

Although there are correlations between $CH_4$ and $CO_2$ at LAN, the different source/sink regimes may induce bias on the regional $CO_2$ estimation in the AUX method, typically in summer. On the other hand, the atmospheric $CH_4$ and $CO_2$ at LAN are not perfectly correlated, meaning that some $CO_2$ events cannot be determined by the $CH_4$ mole fractions.

Relatively, there is less disadvantages in the MET method for the data selection. As this method mainly focuses on the influence of potential local sources and sinks and considers diurnal variations, local topography, and meteorological conditions, it is reasonable to identify the influence of local sources and sinks and is suitable to be applied at other regional stations. However, we have to mention that, due to the intake height (only 10 m a.g.l.) in this study and the complex influence of the land biosphere, the data selected at LAN may not fully represent the volume in regional scale. Although we selected the data from 10:00 to 16:00 LT when the boundary layer is the highest and the surface wind speed was faster than 1.5 $m\,s^{-1}$, the influence of local land biosphere could not be fully eliminated. This influence can be seen from the frequently lower $CO_2$ mole fraction at 10 m a.g.l. than 50 m a.g.l. during daytime in summer. Moreover, due to the different characteristics and source/sink regimes of various gas species, the suitability of a particular filtering method may even differ when looking at different trace gases at the same sampling site. However, this needs to be studied separately.

*Acknowledgements.* We express our great thanks to the staff at Lin'an station, who have contributed to the system installation and maintenance at the stations. This work is supported by National Natural Science Foundation of China (No. 41375130, 41175116, 41405129). Martin Steinbacher acknowledges funding from QA/SAC Switzerland which is financially supported by MeteoSwiss and Empa.

## References

AGGI: The NOAA Annual Greenhouse Gas Index (AGGI), available at: http://esrl.noaa.gov/gmd/aggi/aggi.html (last access: 3 July 2015), 2014.

Artuso, F., Chamard, P., Piacentino, S., Sferlazzo, D. M., Silvestri, L. D., Sarra, A. D., Meloni, D., and Monteleone, F.: Influence of transport and trends in amtospheric $CO_2$ at Lampedusa, Atmos. Environ., 43, 3044–3051, doi:10.1016/j.atmosenv.2009.03.027, 2009.

Baumgardner, D., Raga, G., Peralta, O., Rosas, I., Castro, T., Kuhlbusch, T., John, A., and Petzold, A.: Diagnosing black carbon trends in large urban areas using carbon monoxide measurements, J. Geophys. Res., 107, 8342, doi:10.1029/2001JD000626, 2002.

Brunke, E. G., Labuschagne, C., Parker, B., Scheel, H. E., and Whittlestone, S.: Baseline air mass selection at Cape Point, South Africa: application of $^{222}$Rn and other filter criteria to $CO_2$, Atmos. Environ., 38, 5693–5702, doi:10.1016/j.atmosenv.2004.04.024, 2004.

Cape, J. N., Methven, J., and Hudson, L. E.: The use of trajectory cluster analysis to interpret trace gas measurements at Mace Head, Ireland, Atmos. Environ., 34, 3651–3663, doi:10.1016/S1352-2310(00)00098-4, 2000.

Cape, J. N., Coyle, M., and Dumitrean, P.: The atmospheric lifetime of black carbon, Atmos. Environ., 59, 256–263, doi:10.1016/j.atmosenv.2012.05.030, 2012.

CDIAC: Carbon Dioxide Information Analysis Center, available at: http://cdiac.ornl.gov/trends/emis/meth_reg.html (last access: 29 June 2015), 2015.

Chen, H., Winderlich, J., Gerbig, C., Hoefer, A., Rella, C. W., Crosson, E. R., Van Pelt, A. D., Steinbach, J., Kolle, O., Beck, V., Daube, B. C., Gottlieb, E. W., Chow, V. Y., Santoni, G. W., and Wofsy, S. C.: High-accuracy continuous airborne measurements of greenhouse gases

($CO_2$ and $CH_4$) using the cavity ring-down spectroscopy (CRDS) technique, Atmos. Meas. Tech., 3, 375–386, doi:10.5194/amt-3-375-2010, 2010.

Chevallier, F., Deutscher, N. M., Conway, T. J., Ciais, P., Ciattaglia, L., Dohe, S., Fröhlich, M., Gomez-Pelaez, A. J., Griffith, D., Hase, F., Haszpra, L., Krummel, P., Kyrö, E., Labuschagne, C., Langenfelds, R., Machida, T., Maignan, F., Matsueda, H., Morino, I., Notholt, J., Ramonet, M., Sawa, Y., Schmidt, M., Sherlock, V., Steele, P., Strong, K., Sussmann, R., Wennberg, P., Wofsy, S., Worthy, D., Wunch, D., and Zimnoch, M.: Global $CO_2$ fluxes inferred from surface air-sample measurements and from TCCON retrievals of the $CO_2$ total column, Geophys. Res. Lett., 38, L24810, doi:10.1029/2011GL049899, 2011.

Chmura, L., Rozanski, K., Necki, J. M., Zimonch, M., Korus, A., and Pycia, M.: Atmospheric concentrations of carbon dioxide in southern Poland: comparison of mountain and urban environments, Pol. J. Environ. Stud., 17, 859–867, 2008.

Colby, W. H., Crook, F. W., and Webb, S. E. H.: Agricultural Statistics of the People's Republic of China, US Department of Agriculture, Washington, D.C., 1992.

Collaud Coen, M., Weingartner, E., Furger, M., Nyeki, S., Prévôt, A. S. H., Steinbacher, M., and Baltensperger, U.: Aerosol climatology and planetary boundary influence at the Jungfraujoch analyzed by synoptic weather types, Atmos. Chem. Phys., 11, 5931–5944, doi:10.5194/acp-11-5931-2011, 2011.

Conway, T. J., Steele, L. P., and Novelli, P. C.: Correlations among atmospheric $CO_2$, $CH_4$ and CO in the Arctic, March 1989, Atmos. Environ., 27, 2881–2894, doi:10.1016/0960-1686(93)90319-T, 1989.

Cooke, W. F. and Wilson, J. J. N.: A global black carbon aerosol model, J. Geophys. Res., 101, 19395–19409, doi:10.1029/96JD00671, 1996.

Crosson, E. R.: A cavity ring-down analyzer for measuring atmospheric levels of methane, carbon dioxide, and water vapor, Appl. Phys. B-Lasers O., 92, 403–408, doi:10.1007/s00340-008-3135-y, 2008.

Cunnold, D. M., Steele, L. P., Fraser, P. J., Simmonds, P. G., Prinn, R. G., Weiss, R. F., Porter, L. W., O'Doherty, S., Langenfelds, R. L., Krummel, P. B., Wang, H. J., Emmons, L., Tie, X. X., and Dlugokencky, E. J.: In situ measurements of atmospheric methane at GAGE/AGAGE sites during 1985–2000 and resulting source inferences, J. Geophys. Res., 107, 4225, doi:10.1029/2001JD001226, 2002.

Dlugokencky, E. J., Steele, L. P., Lang, P. M., and Masarie, K. A.: Atmospheric $CH_4$ at Mauna Loa and Barrow Observatories: presentation and analysis of in in situ measurements, J. Geophys. Res., 100, 23103–23113, doi:10.1029/95jd02460, 1995.

Draxler, R. R. and Rolph, G. D.: YSPLIT (HYbrid Single-Particle Lagrangian Integrated Trajectory), NOAA Air Resources Laboratory, Silver Spring, MD, available at: http://www.arl.noaa.gov/ready/hysplit4.html (last access: 3 July 2015), 2003.

Fang, S. X., Zhou, L. X., Zang, K. P., Wang, W., Xu, L., Zhang, F., Yao, B., Liu, L. X., and Wen, M.: Measurement of atmospheric $CO_2$ mixing ratio by cavity ring-down spectroscopy (CRDS) at the 4 background stations in China, Acta Scientiae Circumstantiae, 31, 624–629, 2011 (in Chinese).

Fang, S. X., Zhou, L. X., Masarie, K. A., Xu, L., and Rella, C. W.: Study of atmospheric $CH_4$ mole fractions at three WMO/GAW stations in China, J. Geophys. Res., 118, 4874–4886, doi:10.1002/jgrd.50284, 2013.

Fang, S. X., Zhou, L. X., Tans, P. P., Ciais, P., Steinbacher, M., Xu, L., and Luan, T.: In situ measurement of atmospheric $CO_2$ at the four WMO/GAW stations in China, Atmos. Chem. Phys., 14, 2541–2554, doi:10.5194/acp-14-2541-2014, 2014.

Feng, J., Zhong, M., Xu, B., Du, Y., Wu, M., Wang, H., and Chen, C.: Concentrations, seasonal and diurnal variations of black carbon in $PM_{2.5}$ in Shanghai, China, Atmos. Res., 147–148, 1–9, doi:10.1016/j.atmosres.2014.04.018, 2014.

Greally, B. R., Manning, A. J., Reimann, S., McCulloch, A., Huang, J., Dunse, B. L., Simmonds, P. G., Prinn, R. G., Fraser, P. J., Cunnold, D. M., O'Doherty, S., Porter, L. W., Stemmler, K., Vollmer, M. K., Lunder, C. R., Schmidbauer, N., Hermansen, O., Arduini, J., Salameh, P. K., Krummel, P. B., Wang, R. H. J., Folini, D., Weiss, R. F., Maione, M., Nickless, G., Stordal, F., and Derwent, R. G: Observations of 1,1-difluoroethane (HFC-152a) at AGAGE and SOGE monitoring stations in 1994–2004 and derived global and regional emission estimates, J. Geophys. Res., 112, D06308, doi:10.1029/2006JD007527, 2007.

Gregg, J. S., Andres, R. J., and Marland, G.: China: emissions pattern of the world leader in $CO_2$ emissions from fossil fuel consumption and cement production, Geophys. Res. Lett., 35, L08806, doi:10.1029/2007GL032887, 2008.

Jamali, H., Livesley, S. J., Hutley, L. B., Fest, B., and Arndt, S. K.: The relationships between termite mound $CH_4/CO_2$ emissions and internal concentration ratios are species specific, Biogeosciences, 10, 2229–2240, doi:10.5194/bg-10-2229-2013, 2013.

Keeling, C. D.: Global observations of atmospheric $CO_2$, in: The Global Carbon Cycle, edited by: Heimann, M., NATO ASI Series, vol. 15, Springer, New York, 1–30, 1993.

Keeling, C. D., Bacastow, R. B., Bainbridge, A., Ekdahl Jr., C. A., Guenther, P. R., Waterman, L. S., and Chin, J. F.: Atmospheric carbon dioxide variations at Mauna Loa Observatory, Hawaii, Tellus, 28, 538–551, 1976.

Le Quéré, C., Andres, R. J., Boden, T., Conway, T., Houghton, R. A., House, J. I., Marland, G., Peters, G. P., van der Werf, G. R., Ahlström, A., Andrew, R. M., Bopp, L., Canadell, J. G., Ciais, P., Doney, S. C., Enright, C., Friedlingstein, P., Huntingford, C., Jain, A. K., Jourdain, C., Kato, E., Keeling, R. F., Klein Goldewijk, K., Levis, S., Levy, P., Lomas, M., Poulter, B., Raupach, M. R., Schwinger, J., Sitch, S., Stocker, B. D., Viovy, N., Zaehle, S., and Zeng, N.: The global carbon budget 1959–2011, Earth Syst. Sci. Data, 5, 165–185, doi:10.5194/essd-5-165-2013, 2013.

Liu, L., Zhou, L., Zhang, X., Wen, M., Zhang, F., Yao, B., and Fang, S.: The characteristics of atmospheric $CO_2$ concentration variation of the four national background stations in China, Sci. China Ser. D, 52, 1857–1863, 2009.

Lu, W. F., Chen, W., Duan, B. W., Guo, W. M., Lu, Y., Lantin, R. S., Wassmann, R., and Neue, H. U.: Methane emissions and mitigation options in irrigated rice fields in southeast China, Nutr. Cycl. Agroecosys., 58, 65–73, 2000.

Manning, A. J., O'Doherty, S., Jones, A. R., Simmonds, P. G., and Derwent, R. G.: Estimating UK methane and nitrous oxide emissions from 1990 to 2007 using an inversion modeling approach, J. Geophys. Res., 116, D02305, doi:10.1029/2010JD014763, 2011.

Massen, F. and Beck, E. G.: Accurate estimation of $CO_2$ background level from near ground measurements at non-mixed environments, in: The Economic, Social and Political Elements of Climate Change: Climate Change Management, Springer, Berlin, Heidelberg, 509–522, 2011.

Marland, G.: Emissions accounting: China's uncertain $CO_2$ emissions, Nat. Clim. Chang., 2, 645–646, doi:10.1038/nclimate1670, 2012.

MBL: OAA Greenhouse Gas Marine Boundary Layer Reference, available at: http://esrl.noaa.gov/gmd/ccgg/mbl/data.php (last access: 3 July 2015), 2015.

Morimoto, S., Nakazawa, T., Aoki, S., Hashida, G., and Yamanouchi, T.: Concentration variations of atmospheric $CO_2$ observed at Syowa Station, Antarctica from 1984 to 2000, Tellus B, 55, 170–177, doi:10.1034/j.1600-0889.2003.01471.x, 2003.

Moore III, B. and Braswell, B. H.: The lifetime of excess atmospheric carbon dioxide, Global Biogeochem. Cy., 8, 23–38, doi:10.1029/93GB03392, 1994.

National Bureau of Statistics: 2010 Sixth national population census data Gazette (No.1), Conference Press, April 28, Beijing, China, 2011.

Necki, J., Schmidt, M., Rozanski, K., Zimnoch, M., Korus, A., Lasa, J., Graul, R., and Levin, I.: Six-year record of atmospheric carbon dioxide and methane at a high-altitude mountain site in Poland, Tellus B, 55, 94–104, doi:10.1034/j.1600-0889.2003.01446.x, 2003.

Nevison, C. D., Mahowald, N. M., Doney, S. C., Lima, I. D., van der Werf, G. R., Randerson, J. T., Baker, D. F., Kasibhatla, P., and McKinley, G. A.: Contribution of ocean, fossil fuel, land biosphere, and biomass burning carbon fluxes to seasonal and interannual variability in atmospheric $CO_2$, J. Geophys. Res., 113, G01010, doi:10.1029/2007JG000408, 2008.

Novelli, P. C., Masarie, K. A., Lang, P. M., Hall, B. D., Myers, R. C., and Elkins, J. W.: Reanalysis of tropospheric CO trends: effects of the 1997–1998 wildfires, J. Geophys. Res., 108, 4464, doi:10.1029/2002JD003031, 2003.

Penner, J. E., Eddleman, H., and Novakov, T.: Towards the development of a global inventory for black carbon emissions, Atmos. Environ., 27, 1277–1295, doi:10.1016/0960-1686(93)90255-W, 1993.

Pickers, P. A. and Manning, A. C.: Investigating bias in the application of curve fitting programs to atmospheric time series, Atmos. Meas. Tech., 8, 1469–1489, doi:10.5194/amt-8-1469-2015, 2015.

Prinn, R., Huang, J., Weiss, R., Cunnold, D., Fraser, P., Simmonds, P., McCulloch, A., Harth, C., Salameh, P., O'Doherty, S., Wang, R., Porter, L., and Miller, B.: Evidence for substantial variations of atmospheric hydroxyl radicals in the past two decades, Science, 292, 1882–1888, doi:10.1126/science.1058673, 2001.

Pu, J. J., Xu, H. H., He, J., Fang, S. X., and Zhou, L. X.: Estimation of regional background concentration of $CO_2$ at Lin'an Station in Yangtze River Delta, China, Atmos. Environ., 94, 402–408,doi:10.1016/j.atmosenv.2014.05.060, 2014.

Qin, Y. and Xie, S. D.: Spatial and temporal variation of anthropogenic black carbon emissions in China for the period 1980–2009, Atmos. Chem. Phys., 12, 4825–4841, doi:10.5194/acp-12-4825-2012, 2012.

Repo, M. E., Huttunen, J. T., Naumov, A. V., Chichulin, A. V., Lapshina, E. D., Bleuten, W., and Martikainen, P. J.: Release of $CO_2$ and $CH_4$ from small wetland lakes in western Siberia, Tellus B, 59, 788–796, doi:10.1111/j.1600-0889.2007.00301.x, 2007.

Riley, W. J., Randerson, J. T., Foster, P. N., and Lueker, T. J.: Influence of terrestrial ecosystems and topography on costal $CO_2$ mesurements: a case study at Trinidad Head, California, J. Geophys. Res., 110, g01005, doi:10.1029/2004jg000007, 2005.

Ruckstuhl, A. F., Jacobson, M. P., Field, R. W., and Dodd, J. A.: Baseline subtraction using robust local regression estimation, J. Quant. Spectrosc. Ra., 68, 179–193, doi:10.1016/S0022-4073(00)00021-2, 2001.

Ruckstuhl, A. F., Henne, S., Reimann, S., Steinbacher, M., Vollmer, M. K., O'Doherty, S., Buchmann, B., and Hueglin, C.: Robust extraction of baseline signal of atmospheric trace species using local regression, Atmos. Meas. Tech., 5, 2613–2624, doi:10.5194/amt-5-2613-2012, 2012.

Ryall, D. B., Maryon, R. H., Derwent, R. G., and Simmonds, P. G.: Modelling long-range transport of CFCs to Hace Head, Ireland, Q. J. Roy. Meteor. Soc., 124, 417–446, doi:10.1002/qj.49712454604, 1998.

Ryall, D. B., Derwent, R. G., Manning, A. J., Simmonds, P. G., and O'Doherty, S.: Estimating source regions of European emissions of trace gases from observations at Mace Head, Atmos. Environ., 35, 2507–2523, doi:10.1016/S1352-2310(00)00433-7, 2001.

Sirignano, C., Neubert, R. E. M., Rödenbeck, C., and Meijer, H. A. J.: Atmospheric oxygen and carbon dioxide observations from two European coastal stations 2000–2005: continental influence, trend changes and APO climatology, Atmos. Chem. Phys., 10, 1599–1615, doi:10.5194/acp-10-1599-2010, 2010.

Tans, P. P., Fun, I. Y., and Takahashi, T.: Observation constraints on the global atmospheric $CO_2$ budget, Science, 247, 1431–1438, doi:10.1126/science.247.4949.1431, 1990.

Thompson, R. L., Manning, A. C., Gloor, E., Schultz, U., Seifert, T., Hänsel, F., Jordan, A., and Heimann, M.: In-situ measurements of oxygen, carbon monoxide and greenhouse gases from Ochsenkopf tall tower in Germany, Atmos. Meas. Tech., 2, 573–591, doi:10.5194/amt-2-573-2009, 2009.

Thoning, K. W., Tans, P. P., and Komhyr, W. D.: Atmoshperic carbon dioxide at Mauna Loa observatory 2. Analysis of the NOAA GMCC data, 1974–1985, J. Geophys. Res., 94, 8549–5865, doi:10.1029/JD094iD06p08549, 1989.

Tohjima, Y., Kubo, M., Minejima, C., Mukai, H., Tanimoto, H., Ganshin, A., Maksyutov, S., Katsumata, K., Machida, T., and Kita, K.: Temporal changes in the emissions of $CH_4$ and CO from China estimated from $CH_4/CO_2$ and $CO/CO_2$ correlations observed at Hateruma Island, Atmos. Chem. Phys., 14, 1663–1677, doi:10.5194/acp-14-1663-2014, 2014.

Tsutsumi, Y., Mori, K., Ikegami, M., Tashiro, T., and Tsuboi, K.: Long-term trends of greenhouse gases in regional and background events observed during 1998–2004 at Yonagunijima located to the east of the Asian continent, Atmos. Environ., 40, 2868–5879, 2006.

WMO Greenhouse Gas Bulletin: The state of greenhouse gases in the atmosphere based on global observations through 2011, World Meteorological Organization, Geneva, 2012.

WMO Greenhouse Gas Bulletin: The state of greenhouse gases in the atmosphere based on global observations through 2012, World Meteorological Organization, Geneva 2013.

WMO Greenhouse Gas Bulletin: The state of greenhouse gases in the atmosphere based on global observations through 2013, World Meteorological Organization, Geneva, 2014.

WMO – World Meteorological Organization: WMO World Data Centre for Greenhouse Gases (WDCGG) Data Summary: Greenhouse Gases and Other Atmospheric Gases, No. 37, Japan Meteorological Agency, available at: http://ds.data.jma.go.jp/gmd/wdcgg/pub/products/summary/sum37/sum37contents.html (last access: 11 June 2015), 2013.

Wong, K. W., Fu, D., Pongetti, T. J., Newman, S., Kort, E. A., Duren, R., Hsu, Y.-K., Miller, C. E., Yung, Y. L., and Sander, S. P.: Mapping $CH_4 : CO_2$ ratios in Los Angeles with CLARS-FTS from Mount Wilson, California, Atmos. Chem. Phys., 15, 241–252, doi:10.5194/acp-15-241-2015, 2015.

Worthy, D. E. J., Chan, E., Ishizawa, M., Chan, D., Poss, C., Dlugokencky, E. J., Maksyutov, S., and Levin, I.: Decreasing anthropogenic methane emissions in Europe and Siberia inferred from continuous carbon dioxide and methane observations at Alert, Canada, J. Geophys. Res., 114, D10301, doi:10.1029/2008JD011239, 2009.

Yan, X., Cai, Z., Ohara, T., and Akimoto, H.: Methane emission from rice fields in mainland China: amount and seasonal and spatial distribution, J. Geophys. Res., 108, 4505, doi:10.1029/2002JD003182, 2003.

Zanis, P., Ganser, A., Zellweger, C., Henne, S., Steinbacher, M., and Staehelin, J.: Seasonal variability of measured ozone production efficiencies in the lower free troposphere of Central Europe, Atmos. Chem. Phys., 7, 223–236, doi:10.5194/acp-7-223-2007, 2007.

Zellweger, C., Forrer, J., Hofer, P., Nyeki, S., Schwarzenbach, B., Weingartner, E., Ammann, M., and Baltensperger, U.: Partitioning of reactive nitrogen ($NO_y$) and dependence on meteorological conditions in the lower free troposphere, Atmos. Chem. Phys., 3, 779–796, doi:10.5194/acp-3-779-2003, 2003.

Title Page
Abstract | Introduction
Conclusions | References
Tables | Figures
◀I | ▶I
◀ | ▶
Back | Close
Full Screen / Esc
Printer-friendly Version
Interactive Discussion

Zhang, A., Cui, L., Pan, G., Li, L., Hussain, Q., Zhang, X, Zheng, J., and Crowley, D.: Effect of biochar amendment on yield and methane and nitrous oxide emissions from a rice paddy from Tai Lake plain, China, Agr. Ecosyst. Environ., 139, 469–475, 2010.

Zhang, F., Zhou, L. X., and Xu, L.: Temporal variation of atmospheric $CH_4$ and the potential source regions at Waliguan, China, Sci. China Ser. D, 56, 727–736, doi:10.1007/s11430-012-4577-y, 2013.

Zhang, X., Nakazawa, T., Ishizawa, M., Aoki, S., Nakaoka, H., Sugawara, S., Maksyutov, S., Saeki, T., and Hayasaka, T.: Temporal variations of atmospheric carbon dioxide in the southernmost part of Japan, Tellus, 59, 654–663, doi:10.1111/j.1600-0889.2007.00288.x, 2007.

Zhao, C. L. and Tans, P. P.: Estimating uncertainty of the WMO mole fraction scale for carbon dioxide in air, J. Geophys. Res., 111, D08S09, doi:10.1029/2005JD006003, 2006.

Zhou, L., Conway, T. J., White, J. W. C., Mukai, H., Zhang, X., Wen, Y., Li, J., and MacClune, K.: Long-term record of atmospheric $CO_2$ and stable isotopic ratios at Waliguan Observatory: background features and possible drivers, 1991–2002, Global Biogeochem. Cy., 19, GB2001, doi:10.1029/2004GB002430, 2005.

Zhou, L. X., Worthy, D. E. J., Lang, P. M., Ernst, M. K., Zhang, X. C., Wen, Y. P., and Li, J. L.: Ten years of atmospheric methane observations at a high elevation site in Western China, Atmos. Environ., 38, 7041–7054, 2004.

**Table 1.** The annual regional $CO_2$ mole fractions by the four methods from 2009 to 2011.

| Year | BC (ppm) | REBS (ppm) | AUX (ppm) | MET (ppm) |
|---|---|---|---|---|
| 2009 | 398.9 ± 0.1 | 401.5 ± 0.2 | 398.6 ± 0.2 | 398.6 ± 0.2 |
| 2010 | 402.0 ± 0.1 | 403.7 ± 0.2 | 400.8 ± 0.2 | 401.7 ± 0.2 |
| 2011 | 402.7 ± 0.2 | 407.4 ± 0.2 | 405.1 ± 0.2 | 404.9 ± 0.2 |

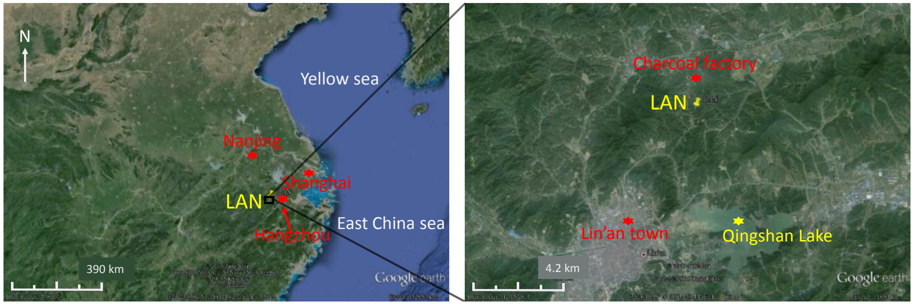

**Figure 1.** Geographic map of the LAN station. The red stars denote cities or towns near the station. The yellow star indicates the Qingshan Lake nearby.

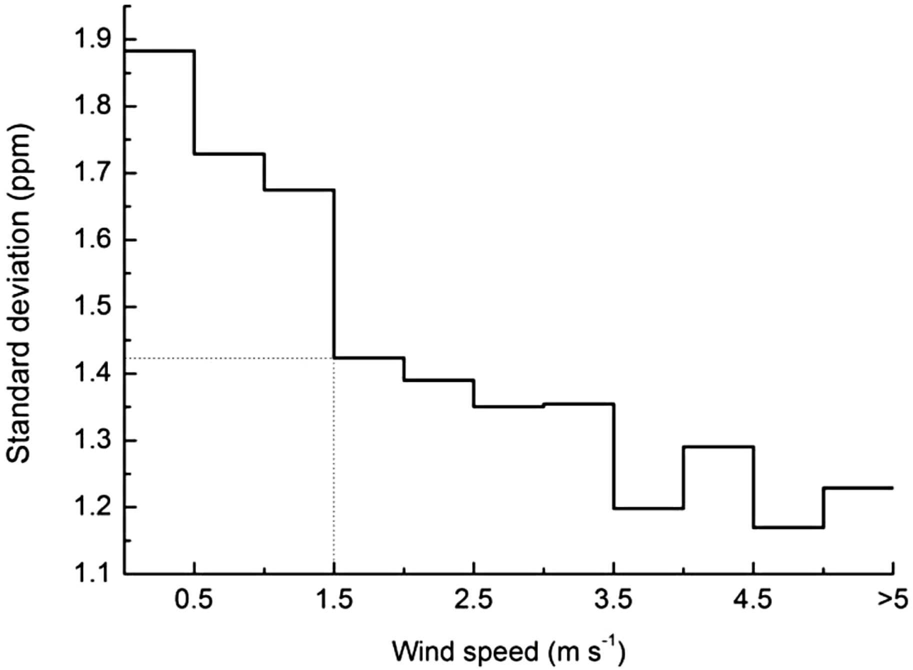

**Figure 2.** Average standard deviations of hourly $CO_2$ mole fractions vs. wind speed based on all data from 10:00 to 16:00 LT from 2009 to 2011. The standard deviations of hourly $CO_2$ data were calculated based on the 5 min segments.

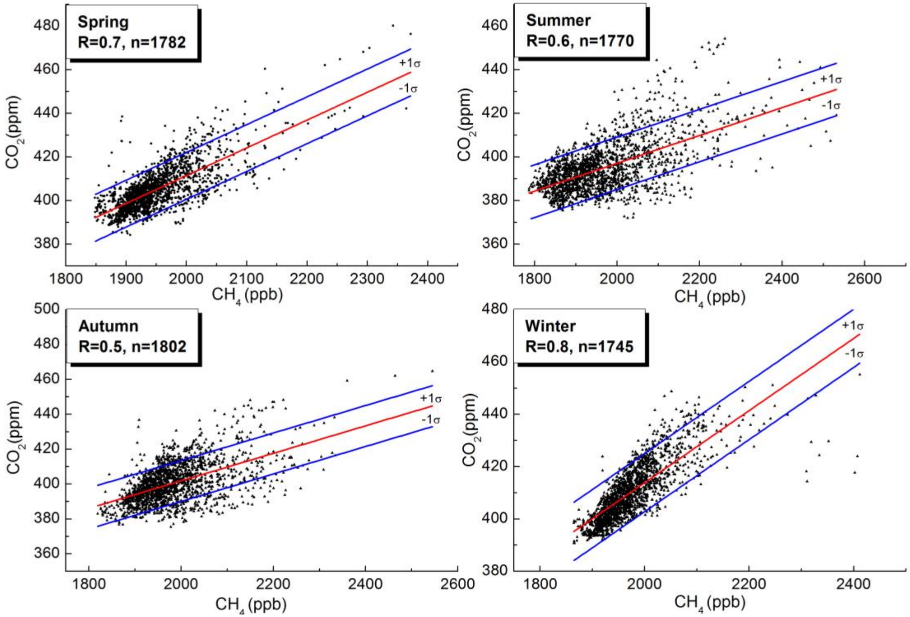

**Figure 3.** Correlations between $CH_4$ and $CO_2$ mole fractions based on all data from 10:00 to 16:00 LT at LAN station. Spring: March–May; Summer: June–August; Autumn: September–November; Winter: December–next February The red lines are linear fits to between the $CH_4$ and $CO_2$ mole fractions. The blue lines in each chart bracket the $CO_2$ values within $\pm 1\sigma$ of the data from 10:00 to 16:00 LT in each season.

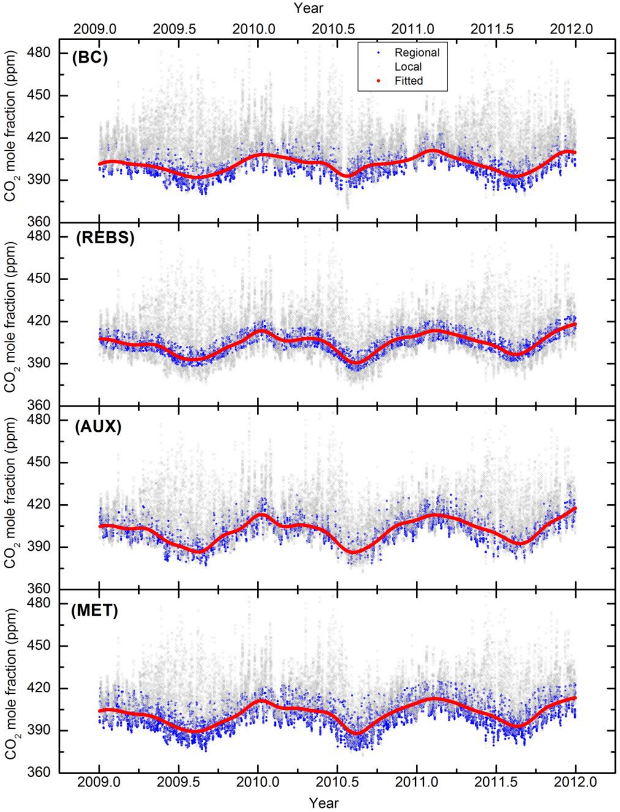

**Figure 4.** Filtered $CO_2$ mole fractions in the four approaches (BC: black carbon as tracer; REBS: Robust Extraction of Baseline Signal; AUX: $CH_4$ as auxiliary tracer; MET: meteorological filter). The closed blue circles represent the filtered regional events. The open grey circles represent local events which are influenced by very local sources or sinks. The red lines are fitted results to the filtered regional events using the curve-fitting method by Thoning et al., (1989).

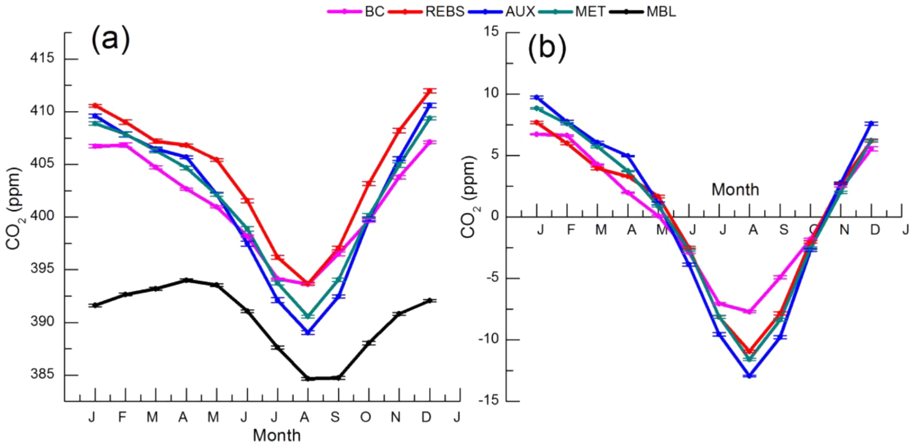

**Figure 5. (a)** Variations of monthly $CO_2$ mole fractions in the four methods. Also compared to the surface values at similar latitudes (30° N) from the MBL reference (Conway et al., 2012). The data in this figure are smoothed values by the curve-fitting method of Thoning et al. (1989). **(b)** The detrended seasonal $CO_2$ cycles in the four methods. This is the smooth curve minus the trend. Error bars indicates confidence intervals of 95 %.

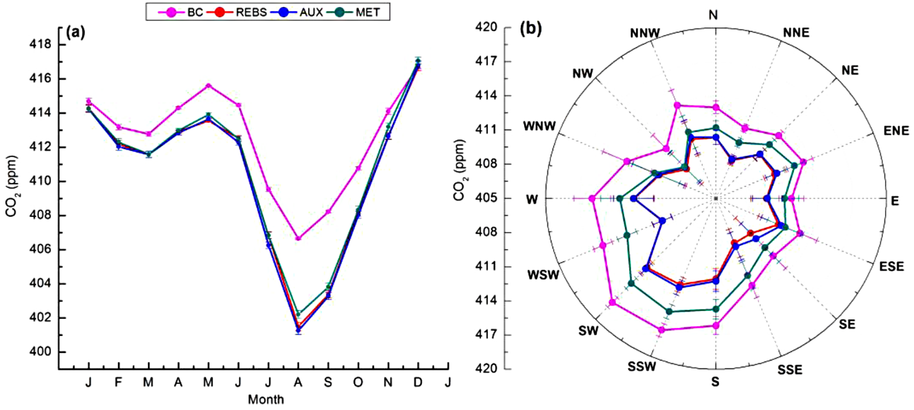

**Figure 6. (a)** Variations of locally influenced $CO_2$ mole fractions in four methods. The data are smoothed $CO_2$ mole fractions by the curve-fitting method of Thoning et al. (1989). **(b)** Wind-rose distribution of locally influenced $CO_2$ mole fractions by the four approaches at LAN. Error bars indicates confidence intervals of 95 %.

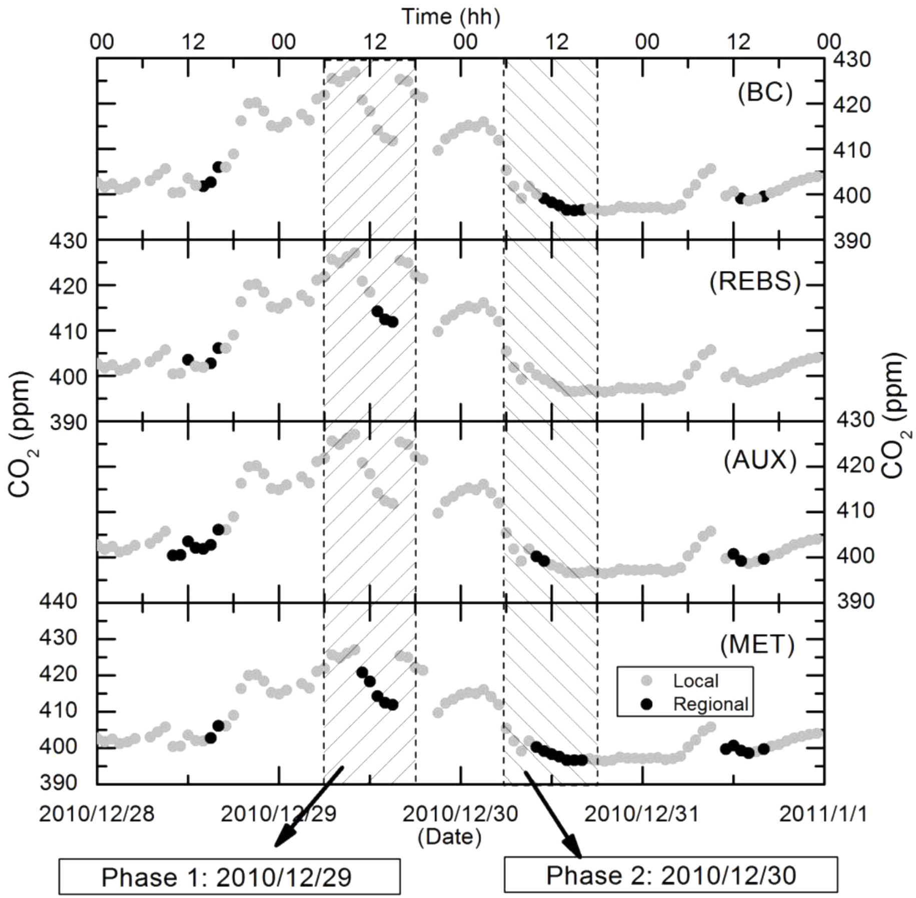

**Figure 7.** The filtered regional and local CO$_2$ mole fractions from 28 December 2010 to 31 December 2010 (LT). The black dots represent the regional events and the grey dots denote the local events. The phase 1 and phase 2 represent periods from 06:00 to 16:00 LT in 29 December 2010 and 30 December 2010, respectively.

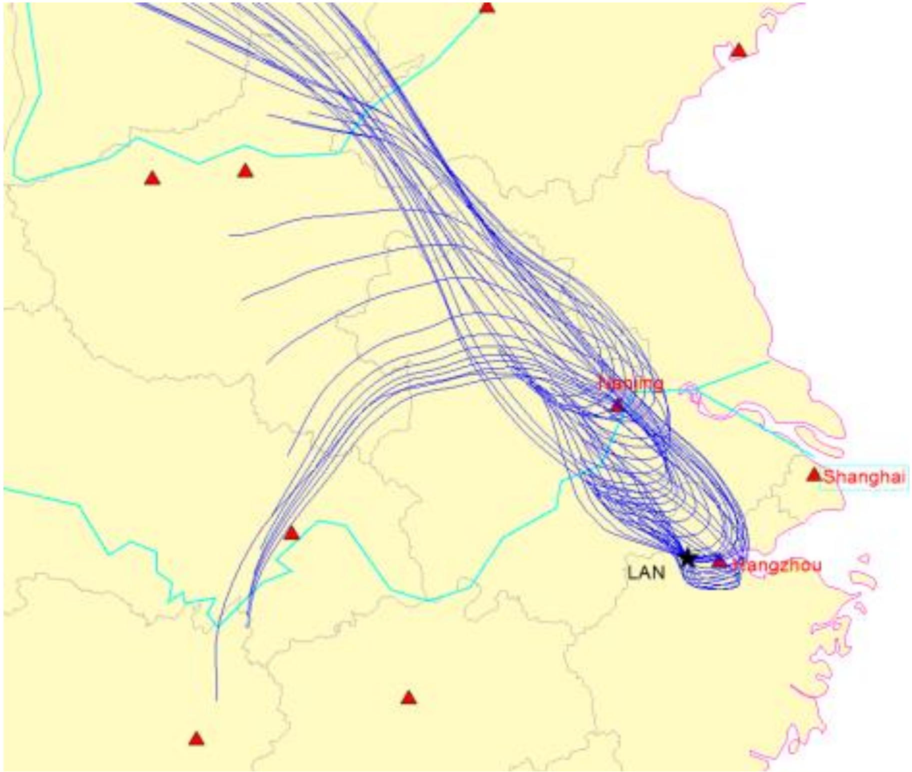

**Figure 8.** HYSPLIT 72 h back trajectories for every hour during 28 December 2010 19:00 LT to 30 December 2010 06:00 LT.